

ON THE MODELING OF GRASPS WITH A MULTI-FINGERED HAND

V. BRODSKY AND M. SHOHAM
Technion - Israel Institute of Technology
Department of Mechanical Engineering
Technion City, Haifa 32000, Israel

Abstract

This research investigates the stability of planar grasps with a multi-fingered robotic hand, using energy approach and geometric interpretation. A more general non-linear finger model was adopted, which reveals that the conditions for stability, obtained by traditional linearized model, are too relaxed.

Geometrically, the critical conditions for the linearized planar model constitute a hyper-plane in the space of grasping forces, whereas the non-linearized model constitutes a third-order surface contained within the permissible region of the former. Hence, allowable grasping forces calculated by a linearized model may practically lead to instability.

The linearized finger model analysis shows that at critical force there is one and only one instantaneous instability center fixed in the plane (which coincides with the compliance center during loading), infinitesimal rotation about which causes instability. When a non-linearized finger model is considered, the compliance center position depends on the applied forces and it moves in the plane during loading. Furthermore, in some cases, there appear a set of instantaneous instability centers as the critical level of forces is reached.

1. Introduction

Within the wide scope of artificial hand design and grasp analysis, this paper concentrates on the subject of grasp stability, which by itself has already been dealt with before by many investigators [Hanafusa and Asada, 1977; Cutkosky, 1985; Mason and Salisbury, 1985; Kerr and Roth, 1986; Li and Sastry, 1987; Nguyen, 1988; Grupen, Henderson, and McCammon, 1989]. In our analysis we use the grasp stability definition of the first approach, given qualitatively by Cutkosky and Howe [in Venkataraman, 1990]: Will the grasp return to its initial configuration after being disturbed by an external force or moment?

We deal in this investigation with a quasi static case which provides the necessary conditions for a stable grasp in the above mentioned sense. (An analysis of the Liapunov stability of a grasp, that takes into consideration also dynamic and control effects, can be found in e.g. [Jen, Shoham, and Longman, 1994]).

The present work compares the model of a 'spring-like' finger as introduced in previous investigations by Hanafusa and Asada [1977], Nguyen [1985b], Cutkosky [1985] and others, with a more comprehensive one which takes into consideration infinitesimal change of finger orientation due to a disturbance, and hence involves second-order terms. This rigorous analysis shows that the linearized finger model cannot be used to determine

practically the region of stable grasping force and the location of the grasp compliance center.

To formulate the problem we made the following assumptions:

- rigid object and fingers,
- finger-object contact is a point one with friction,
- the fingers act as 'spring-like' fingers, namely, force applied at the fingertips is the sum of a given initial force and a disturbance force which is negatively proportional to the fingertip displacement.
- the object is initially in equilibrium.

The goal of this investigation is to calculate, under these assumptions, the boundaries of the grasping forces within which the grasp is stable.

2. Finger Models

Consider a robot hand with four-jointed fingers grasping an object as shown in Figs. 1 and 2. If fingertip motions and forces applied by the finger to the object are in the same plane (the shaded area in Fig. 1), one can equivalently describe the finger behavior in this plane with only a two-jointed finger. This simplification reduces the problem to a planar one, and it is used throughout the paper.

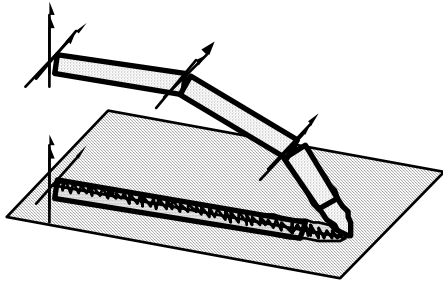


Fig. 1. Projection of a spatial finger on the plane

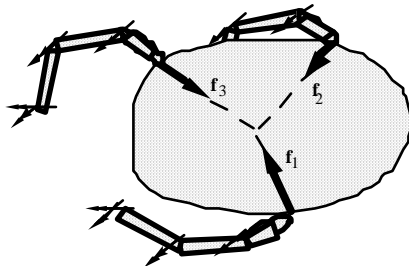


Fig. 2. Body grasped by a three-fingered hand

The 'spring-like' finger model contains at each joint a spring which models the flexibility of the controller (proportional terms) and transmission elasticity. The four-hinge jointed finger model contains four torsional springs, whereas its planar simplification contains only two - one torsional and one linear - as shown in Fig. 3.

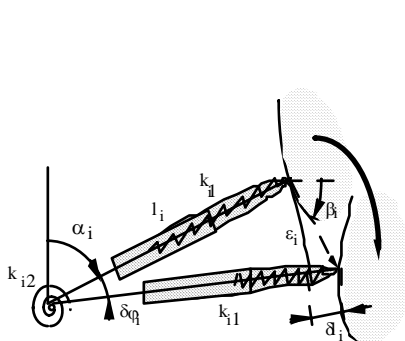


Fig. 3. Planar two DOF finger

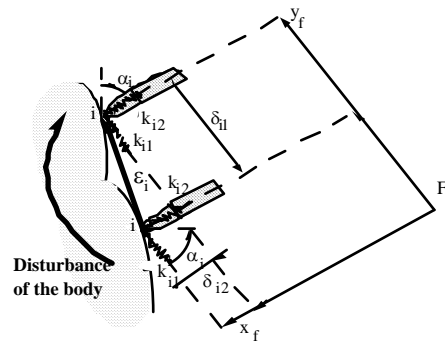


Fig. 4. Linearized finger tip displacement

Previous investigations assumed that infinitesimal motion of the fingertip is negligible compared to the finite length of the finger, namely, following a disturbance the finger still maintains its orientation. Noting that stability analysis requires investigation of the second derivative of energy, it implies that infinitesimal terms must be kept up to the second order. As a result, infinitesimal orientational changes in hinged-finger due to infinitesimal motion of the object cannot be neglected.

2.1. LINEARIZED FINGER MODEL

Starting with the linearized model, Fig. 4, we attach a coordinate system x_f, y_f to the fingertip along which spring deformations are measured. As depicted in Fig. 5, linear translation of the object along a line directed to β_i , causes the fingertip to move from position i to i' , which, in turn, cause spring deflections, δ_{i1}, δ_{i2} given by:

$$\delta_{i1} = \varepsilon_i \cos(\beta_i - \alpha_i), \quad \delta_{i2} = \varepsilon_i \sin(\beta_i - \alpha_i), \quad (1)$$

where ε_i is the i -th fingertip motion (also object motion at i -th fingertip contact point), α_i is the initial finger orientation, and compression is assumed to be positive.

At this point we represent a general displacement of a rigid body in a plane by its two linear and one rotational components. In Section 3, where the concept of instantaneous instability center is introduced, this motion is represented as only a rotation about some point. Hence, object disturbance is written as: $\mathbf{p} = [\delta a \quad \delta b \quad \delta \theta]^T$.

Fingertip displacements, α_i , due to small disturbance, \mathbf{p} , are given in x - y system by :

$$\varepsilon_{ix} = r_i [\cos(\gamma_i + \delta\theta) - \cos \gamma_i] + \delta a, \quad \varepsilon_{iy} = r_i [\sin(\gamma_i + \delta\theta) - \sin \gamma_i] + \delta b. \quad (2)$$

where r_i is the length of a radius-vector from the center of rotation to fingertip i , and γ is the angle of this radius-vector with respect to the hand coordinate system. We use these relations and Eq. (1) to calculate the grasp energy Hessian matrix of the linearized model, U_i , the vanishing of its determinant implies instable grasp.

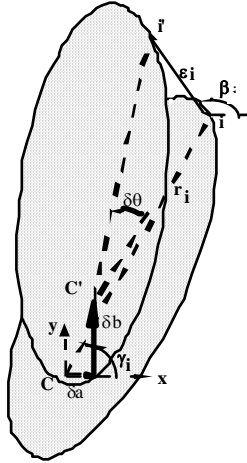


Fig. 5. Object Displacement

Hence, the grasp becomes unstable when: $\det \left[\frac{\partial^2 U_i}{\partial \delta_n \partial \delta_m} \right] = 0$ (3)

where $\partial \delta_n$ and $\partial \delta_m$ are two out of three components of planar disturbance.

Fig. 6. The instability planes

Investigating the components of the Hessian matrix, one can observe that out of nine elements only one, $U_{i,33}$, depends on the initial deflections (initial grasping forces), and this dependency is expressed in a linear manner. In addition, equilibrium equations contribute three other linear equations, resulting in a linear equation in $2N-3$ parameters, which geometrically describes a hyper-plane. In the case of a three-fingered hand ($N=3$), this set of equations is a function of only three components, which implies that instability occurs on a plane in the three-dimensional space of independent deflections.

2.2 NON-LINEARIZED FINGER MODEL

A more accurate non-linearized finger model of a hinge-jointed finger is considered next where each finger contains schematically, one linear and one torsional spring (rather than two linear springs) as shown in Fig. 3. In this case the orientation of the finger due to a small disturbance changes. Springs deflections due to small displacement of the fingertip are:

$$\delta\varphi_i = \tan^{-1} \frac{\varepsilon_i \sin \beta_i}{\ell_i + \varepsilon_i \cos \beta_i}, \quad \delta\ell_i = \left\{ \left[\ell_i + \varepsilon_i \cos \beta_i \right]^2 + \left[\varepsilon_i \sin \beta_i \right]^2 \right\}^{1/2} - \ell_i. \quad (4)$$

where $\delta\varphi_i$ is the change in i -th finger orientation, ℓ_i is its length, and $\delta\ell_i$ is the change in its length. This leads to the following energy Hessian matrix of the non-linearized finger model:

$$U_{j11} = \sum_{i=1}^N \left\{ k_{i1} \cos^2 \alpha_i + k_{i2} \frac{\sin^2 \alpha_i}{\ell_i^2} - k_{i1} \Delta_i \frac{\sin^2 \alpha_i}{\ell_i} - 2k_{i2} \Phi_i \frac{\sin \alpha_i \cos \alpha_i}{\ell_i} \right\}, \quad (5a)$$

$$U_{j12} = U_{i,21} = \sum_{i=1}^N \left\{ \frac{1}{2} \sin 2\alpha_i \left(k_{i1} - \frac{k_{i2}}{\ell_i^2} \right) + k_{i1} \Delta_i \frac{\sin \alpha_i \cos \alpha_i}{\ell_i} + k_{i2} \Phi_i \frac{\cos 2\alpha_i}{\ell_i^2} \right\}, \quad (5b)$$

$$U_{j22} = \sum_{i=1}^N \left\{ k_{i1} \sin^2 \alpha_i + k_{i2} \frac{\cos^2 \alpha_i}{\ell_i^2} - k_{i1} \Delta_i \frac{\cos^2 \alpha_i}{\ell_i} + 2k_{i2} \Phi_i \frac{\sin \alpha_i \cos \alpha_i}{\ell_i} \right\}, \quad (5c)$$

$$U_{j13} = U_{j,31} = \sum_{i=1}^N \left\{ -r_i \left[k_{i1} \cos \alpha_i \sin(\gamma_i - \alpha_i) + k_{i2} \frac{\sin \alpha_i \cos(\gamma_i - \alpha_i)}{\ell_i^2} + k_{i1} \Delta_i \frac{\sin \alpha_i \cos(\gamma_i - \alpha_i)}{\ell_i} + k_{i2} \Phi_i \frac{\cos(\gamma_i - 2\alpha_i)}{\ell_i^2} \right] \right\}, \quad (5d)$$

$$U_{j13} = U_{j,31} = \sum_{i=1}^N \left\{ -r_i \left[k_{i1} \cos \alpha_i \sin(\gamma_i - \alpha_i) + k_{i2} \frac{\sin \alpha_i \cos(\gamma_i - \alpha_i)}{\ell_i^2} + k_{i1} \Delta_i \frac{\sin \alpha_i \cos(\gamma_i - \alpha_i)}{\ell_i} + k_{i2} \Phi_i \frac{\cos(\gamma_i - 2\alpha_i)}{\ell_i^2} \right] \right\}, \quad (5e)$$

$$U_{j13} = U_{j,31} = \sum_{i=1}^N \left\{ -r_i \left[k_{i1} \cos \alpha_i \sin(\gamma_i - \alpha_i) + k_{i2} \frac{\sin \alpha_i \cos(\gamma_i - \alpha_i)}{\ell_i^2} + k_{i1} \Delta_i \frac{\sin \alpha_i \cos(\gamma_i - \alpha_i)}{\ell_i} + k_{i2} \Phi_i \frac{\cos(\gamma_i - 2\alpha_i)}{\ell_i^2} \right] \right\}, \quad (5f)$$

As is expected, all the components of the Hessian matrix depend on the grasping forces (the initial springs deflections) which make the solution of stable grasping forces boundaries more difficult. Actually, after substituting the linear conditions for equilibrium, the equation of critical forces is a third order algebraic equation in $2N-3$ independent deflections (forces).

3. Instantaneous Instability Center (IIC)

The definiteness of the Hessian matrix (and, correspondingly, the stability of grasping) depends on the principal minors of the Hessian. It can be shown that both the first and the second principle minors of the linearized model are always positive (except where all springs' stiffness are zero, which obviously has no physical sense). Observing that all terms composing the first and second principal minors of the Hessian matrix are invariant to coordinate system origin location, one can choose this origin to coincide with the instantaneous center, x_c, y_c , the coordinates of which are obtained, in the linearized case, by

$$\begin{aligned}
 & x_c \frac{1}{2} \sum_i \sin 2\alpha_i (k_{i1} - k_{i2}) - y_c \sum_i (k_{i1} \cos^2 \alpha_i + k_{i2} \sin^2 \alpha_i) = \\
 & = \sum_i \frac{1}{2} x_i (k_{i1} - k_{i2}) \sin 2\alpha_i - \sum_i y_i (k_{i1} \cos^2 \alpha_i + k_{i2} \sin^2 \alpha_i) \\
 & : \\
 & x_c \sum_i (k_{i1} \sin^2 \alpha_i + k_{i2} \cos^2 \alpha_i) - y_c \frac{1}{2} \sum_i \sin 2\alpha_i (k_{i1} - k_{i2}) = \\
 & = \sum_i x_i (k_{i1} \sin^2 \alpha_i + k_{i2} \cos^2 \alpha_i) - \sum_i \frac{1}{2} y_i (k_{i1} - k_{i2}) \sin 2\alpha_i
 \end{aligned} \tag{6}$$

It is helpful to note that the determinant of the above system is the same second order minor of the Hessian matrix and it is always positive. It follows that system (6) has a solution for all grasps, and this solution is unique. In the case of a linearized finger model, such a solution is also independent of the initial deflections of the springs, or equivalently, of initial grasping forces. Consequently, since the determinant of (6) is always positive (and cannot vanish), the instantaneous instability center (IIC), i.e., the point about which the object rotate once instability occur, does not lie at infinity. It means that instability of grasp with linearized finger model is caused by a rotation, and not by pure translation (rotation about point at infinity).

When grasp compliance is considered, the same point coincides with the compliance center as was derived by Nguyen [1985] and Shimoga and Goldenberg [1992]. We will demonstrate next that its constant position and uniqueness is, however, not guaranteed for the non-linearized finger model.

4. Force Boundaries for Non-Linearized Finger Model Grasps

Similarly to the linearized model, we also redefine the problem by considering a general disturbance in the plane to be a rotation about some point. One can investigate the occurrence of instability by looking for a center of rotational instability. Hence:

$$\sum_i \left(k_{i1} B_i^2 + \frac{k_{2i}}{\ell_i^2} A_i^2 + k_{i1} \Delta_i \left(-A_i - \frac{A_i^2}{\ell_i} \right) + k_{2i} \Phi_i \left(-\frac{B_i}{\ell_i} - 2 \frac{A_i B_i}{\ell_i^2} \right) \right) = 0 \tag{7}$$

where A_i and B_i are:

$$A_i = (x_i - x_c) \cos \alpha_i + (y_i - y_c) \sin \alpha_i, \quad B_i = -(x_i - x_c) \sin \alpha_i + (y_i - y_c) \cos \alpha_i.$$

It is worth noting that the introduced parameters A_i and B_i are functions of the grasp geometry and unknown IIC coordinates only, and are independent of the disturbance of the object. It enables us to write the derivatives of springs deflection with respect to small rotation of the object, in terms of those parameters.

Eq. (7) delineates the limits of grasp stability in the space of applied forces. It cannot, however, be directly solved since the coefficients of A_i and B_i contain the coordinates of

IIC which are unknown. In order to solve this, we utilize the fact that a set of forces in equilibrium remains in equilibrium after being multiplied by some scalar. This fact enables us to divide the problem into two - one being the geometric property of the grasp while the other, denoted by Force Intensity Level (FIL), is its intensity, .

The coefficients A_i and B_i , are linear functions of IIC's coordinates. Hence, the second derivative of the energy is a quadratic form of x_c and y_c . It is also possible to separate the coefficients into two expressions - a_{ij} , that contains only geometrical properties of the grasp and stiffness of the springs; and - b_{ij} , that contains the initial grasping forces (springs' deflections), which we assume to be normalized and in equilibrium. Writing the second derivative of energy in such a form yields:

$$\begin{aligned} \frac{d^2U}{d(\delta\theta)^2} \Big|_{\delta\theta=0} &= (a_{11} - t \cdot b_{11})x_c^2 + 2(a_{12} - t \cdot b_{12})x_c y_c + (a_{22} - t \cdot b_{22})y_c^2 + \\ &2(a_{13} - t \cdot b_{13})x_c + 2(a_{23} - t \cdot b_{23})y_c + (a_{33} - t \cdot b_{33}) = 0 \end{aligned} \quad (8)$$

where t is FIL. The coefficients of this equation given explicitly in Appendix A.

4.1 GEOMETRIC INTERPRETATION

Consider the second derivative of the energy given in (8), as being a spatial quadratic surface. It can be proven that for small FIL this surface whole lies above the xy plane which physically means a stable grasp. Increasing FIL, t causes stretching of the surface along the z axis until, at a critical force it touches the xy plane. At this point there appears an IIC in the plane the rotation about which cause instability. It is possible, however, that the intersection of the surface with the xy plane occurs along a curve which causes the appearance of a set of IICs the rotation about each causes instability. This differs from the linearized model where only one IIC might exist.

Mathematically, one can consider (8) as a planar quadratic form the behavior of which is fully described by its matrix:

$$\mathbf{A} = \begin{bmatrix} (a_{11} - t \cdot b_{11}) & (a_{12} - t \cdot b_{12}) & (a_{13} - t \cdot b_{13}) \\ (a_{12} - t \cdot b_{12}) & (a_{22} - t \cdot b_{22}) & (a_{23} - t \cdot b_{23}) \\ (a_{13} - t \cdot b_{13}) & (a_{23} - t \cdot b_{23}) & (a_{33} - t \cdot b_{33}) \end{bmatrix}, \quad (9)$$

and its invariants:

$$\mathbf{A}(t) = \begin{bmatrix} (a_{11} - t \cdot b_{11}) & (a_{12} - t \cdot b_{12}) & (a_{13} - t \cdot b_{13}) \\ (a_{12} - t \cdot b_{12}) & (a_{22} - t \cdot b_{22}) & (a_{23} - t \cdot b_{23}) \\ (a_{13} - t \cdot b_{13}) & (a_{23} - t \cdot b_{23}) & (a_{33} - t \cdot b_{33}) \end{bmatrix} \quad (9a)$$

$$\mathbf{D}(t) = \begin{bmatrix} (a_{11} - t \cdot b_{11}) & (a_{12} - t \cdot b_{12}) \\ (a_{12} - t \cdot b_{12}) & (a_{22} - t \cdot b_{22}) \end{bmatrix} \quad (9b) \quad \mathbf{I}(t) = (a_{11} - t \cdot b_{11}) + (a_{22} - t \cdot b_{22}) \quad (9c)$$

Note that for $t=0$, all these invariants are positive, which can easily be proved as follows.

All components of $\mathbf{I}(0)$ are positive (see Appendix A). The expression of $\mathbf{D}(0)$ coincides with the second principal minor of the linearized finger model Hessian matrix, \mathbf{M}_2 , and as was noted earlier, is positive for all grasping configurations. Since the determinant $\mathbf{A}(0)$ is independent of the choice of the coordinate system origin, one may choose such a system that terms a_{13} and a_{23} vanish. In this case $\mathbf{A}(0)$ becomes: $\mathbf{A}(0) = \mathbf{M}_2 \cdot \mathbf{a}'_{33}$, which is positive. Note that positive definiteness of \mathbf{a}'_{33} is obtained for non-zero springs stiffness and for finite object size. The above discussion implies that positive values of invariants (12a-c) assure a stable grasp.

Note that invariants (12a-c) are all continuous functions of FIL, t , since $A(t)$, $D(t)$ and $I(t)$ are, respectively, polynomials of the third, second and first order in t , with constant coefficients. Since the invariants at $t=0$ are all positive and continuous, there exists a region of FIL $0 \leq t \leq t_1$, in which these invariants remain positive. As mentioned above, such positive definiteness of these invariants means a stable grasp. Thus, we have proved the next Theorem:

A planar grasp in equilibrium with one torsional and one linear 'spring-like' fingers with friction, is stable for small grasping forces.

Geometrically, the vanishing of $A(t)$ while $D(t)$ remains positive means that the surface (8) touches the plane in a single point. Further increasing t leads to transformation of this point into an ellipse. Simultaneous vanishing of $A(t)$ and $D(t)$ leads to more complicated cases, such as the appearance of a line or a hyperbola at a critical point. The various cases of instability are illustrated in the next section.

5. Illustrative Example

Two examples, that illustrate the spatial behavior of the energy second derivative of a grasp with non-linearized finger model, are given next. The first example is a symmetrical grasp of a round object. A drawing of the grasped object and corresponding finger data are given in Fig. 7.a. As was proven earlier, $A(t)$ starts from a positive value at $t=0$, and after reaching zero at a critical point, remains negative. In this case the shape is maintained as elliptic paraboloid while crossing the xy plane, which means IIC is a point in the plane. From the view of our geometric analysis this is a typical case, and it is confirmed by Fig. 7c.

The second case is illustrated by Figs. 8a-c. The geometry of the grasp and its parameters are identical to the first case. The only difference is that one normal force is a unit, the two others equal zero. Obviously, considering a circular object, slippage may occur; but we can easily choose an appropriate shape (rectangle, for example), so that the given system of forces will not cause finger slippage. This distribution of forces leads to a different behavior of the invariant $A(t)$. It vanishes at the critical point, but does not change its sign. Still, the invariant $I(t)$ is sufficiently positive, and only the second invariant $D(t)$ defines the form of the intersection curve after the critical point. The negative value of $D(t)$ in addition to the positive $A(t)$ and $I(t)$ means that the curve is a hyperbola.

Geometrically, at the critical point, the intersection of the surface with the xy plane gives two coincided lines. Further increasing FIL leads to transformation of those lines into two branches of hyperbola. The surface of energy second derivative in this case gains infinity curvature in one direction at the critical point, and this curvature becomes negative immediately after the force intensity level exceeds this point.

6. Numerical Solution of the Grasping Force Boundaries

In this section, the algorithm for obtaining the instability surface is presented. For a planar object grasped by three point fingers with friction, there are six interacting forces of which three are dependent through equilibrium equations. Derivation of the surface that bounds stable grasp, takes place in the space of three independent forces where each point in this space describes an equilibrium state.

Increasing the FIL produces a ray in the first octant (for squeezing forces) extending from the origin until at a point t it pierces the stable grasp boundary surface. Each ray in

the space of independent forces can be obtained as a combination of some equilibrium system of forces and intensity, t . There is a one-to-one correspondence between the rays starting at the origin of independent forces' coordinate system and all possible states of equilibrium with the specifically determined metrics - force intensity level.

With this representation, one can solve the equation of instability condition for a given system of forces, or in another words, for a specific ray. The minimal positive root of this equation is the critical force intensity. Note that this is a cubic equation and can be rewritten as follows:

$$A(t) = e_0 t^3 + e_1 t^2 + e_2 t + e_3 = 0, \quad (10)$$

where e_0 , e_1 , e_2 , and e_3 are given in Appendix A.

The critical surfaces in the space of three independent deflections, for linearized and non-linearized finger models, are given in Fig. 6. This is for a symmetrical grasp of a circular object with symmetrical distribution of forces and the same size of object and fingers. The closer-to-origin surface corresponds to the non-linearized finger model. The further one is a plane obtained by the linearized finger model. The comparison of those surfaces leads to the conclusion that the non-linearized model shows instability at about one half of the forces allowed by the linearized model, which is obviously unacceptable for practical applications.

This indicates that only when the dimensions of the fingers are sufficiently larger compared to the object, one can use the formulae for the linearized model to calculate the critical forces. Otherwise, the linearized model conditions allow too high a load and ultimately can lead to instability.

7. Conclusions

The boundaries of grasping forces that maintain stable grasp with 'spring-like' fingers are derived in this paper. Both linearized and more accurate non-linearized finger model are discussed.

It has been shown that critical forces describe a hyper-plane in the space of applied forces when a linearized finger model is used, and a third-order surface when a non-linearized model is used. The critical surface corresponding to the non-linearized finger model lies closer to the origin, and hence permits smaller grasping forces than the surface corresponding to the linearized model. In a common case, when the object and the fingers are of similar sizes, the allowed forces can be as low as half of that calculated by the linearized model.

The linearized finger model leads to a unique point in the plane, the rotation about which has a minimal stiffness (compliance center); and for the critical level of forces the infinitesimal rotation about it leads to instability. In our work where instability is concerned it is termed the instantaneous instability center. An important feature of the compliance center is that its position is function of the geometry of grasp and stiffness of fingers and is independent on the grasping forces.

When the non-linearized model is used, this observation no longer holds. First, the location of the compliance center depends on the forces system applied to the object and can move in the plane during loading. Secondly, in some cases, as the critical force intensity level is reached, a set of instantaneous instability centers may appear.

The use of geometric interpretation of the grasp stability problem, simplifies the calculation of the critical forces. This algorithm requires the solution of a set of cubic equations instead of the investigation of a third-order surface as obtained by evaluating the Hessian matrix of the grasp energy function.

References

- Cutkosky, M. R., *Robotic Grasping and Fine Manipulation*, Kluwer Academic Publishers, Hingham, Massachusetts, 1985.
- Gruppen, R. A., Henderson, T. C. and McCammon, I. D., "A Survey of General Purpose Manipulation," *The Int. Journal of Robotics Research*, Vol. 8, No. 1, pp. 38-62, 1989.
- Hanafusa, H. and Asada, H., "Stable Prehension by a Robot Hand with Elastic Fingers," Proc. of the *7th Int. Symposium on Industrial Robots*, Tokyo, pp. 361-368, 1977.
- Jen, F., Shoham, M. and Longman, R. W., "Liapunov Stability of Force-Controlled Grasps with a Multi-Fingered Hand," to be published in *The Int. Journal of Robotics Research*.
- Kerr, J. and Roth, B., "Analysis of Multifingered Hands," *The Int. Journal of Robotics Research*, Vol. 4, No. 4, pp. 3-17, 1986.
- Li, Z. and Sastry, S., "Task Oriented Optimal Grasping by Multifingered Robot Hands," Proc. of the *IEEE Int. Conference on Robotics and Automation*, Raleigh, pp. 389-394, 1987.
- Mason, M. T. and Salisbury, J. K. Jr., *Robot Hands and the Mechanics of Manipulation*, MIT Press, Cambridge, Massachusetts, 1985.
- Nguyen, V.-D., "The Synthesis of Force-Closure Grasps in the Plane," MIT AI Memo 861, MIT Artificial Intelligence Lab., September, 1985a.
- Nguyen, V.-D., "The Synthesis of Stable Grasps in the Plane," MIT AI Memo 862, MIT Artificial Intelligence Lab, October, 1985b.
- Nguyen, V.-D., "Constructing Force-Closure Grasps," *The International Journal of Robotics Research*, Vol. 7, No. 3, pp. 3-16, 1988.
- Shimoga, K. B. and Goldenberg, A. A., "Constructing Multifingered Grasps to Achieve Admittance Center," Proc. of the *IEEE Int. Conference on Robotics and Automation*, Raleigh, pp. 2296-2301, 1992.
- Venkataraman, S. T. and Iberall, T., *Dextrous Robot Hands*, Springer-Verlag Inc., New York, 1990.

Appendix A.

The coefficients of the second derivative of the grasp energy function in a quadratic form are:

$$a_{11} = \sum_i \left(k_{i1} \sin^2 \alpha_i + k_{i2} \frac{\cos^2 \alpha_i}{\ell_i^2} \right), \quad a_{12} = \sum_i \frac{1}{2} \sin 2\alpha_i \left(-k_{i1} + \frac{k_{i2}}{\ell_i^2} \right),$$

$$a_{22} = \sum_i \left(k_{i1} \cos^2 \alpha_i + k_{i2} \frac{\sin^2 \alpha_i}{\ell_i^2} \right), \quad a_{13} = \sum_i \left(k_{i1} M_i \sin \alpha_i - k_{i2} N_i \frac{\cos \alpha_i}{\ell_i^2} \right),$$

$$a_{23} = \sum_i \left(-k_{i1} M_i \cos \alpha_i - k_{i2} N_i \frac{\sin \alpha_i}{\ell_i^2} \right), \quad a_{33} = \sum_i \left(k_{i1} M_i^2 + k_{i2} N_i^2 \right),$$

where: $M_i = -x_i \sin \alpha_i + y_i \cos \alpha_i$, $N_i = x_i \cos \alpha_i + y_i \sin \alpha_i$.

The coefficients that are depended on the initial deflections of the springs (initial grasping forces) are as follows:

$$b_{11} = \sum_i \left[\left(k_{i1} \Delta_i C_i - 2k_{i2} \Phi_i \frac{S_i}{\ell_i} \right) \frac{C_i}{\ell_i} \right], \quad b_{12} = \sum_i \left[\frac{k_{i1} \Delta_i}{\ell_i} S_i C_i + \frac{k_{i2} \Phi_i}{\ell_i^2} (C_i^2 - S_i^2) \right],$$

$$b_{22} = \sum_i \left[\frac{k_{i1} \Delta_i}{\ell_i} S_i^2 + 2 \frac{k_{i2} \Phi_i}{\ell_i^2} S_i C_i \right], \quad b_{13} = \sum_i \left[-\frac{k_{i1} \Delta_i}{\ell_i} N_i C_i + \frac{k_{i2} \Phi_i}{\ell_i^2} (N_i S_i - M_i C_i) \right],$$

$$b_{23} = \sum_i \left[-\frac{k_{i1}\Delta_i}{\ell_i} N_i S_i - \frac{k_{i2}\Phi_i}{\ell_i^2} (N_i C_i + M_i S_i) \right],$$

$$b_{33} = \sum_i \left[k_{i1}\Delta_i N_i \left(1 + \frac{N_i}{\ell_i} \right) + \frac{k_{i2}\Phi_i M_i}{\ell_i} \left(1 + 2\frac{N_i}{\ell_i} \right) \right].$$

The above expressions are used to derive Eq.(14):

$$e_0 = \begin{vmatrix} b_{11} & b_{12} & b_{13} \\ b_{12} & b_{22} & b_{23} \\ b_{13} & b_{23} & b_{33} \end{vmatrix}, \quad e_1 = \begin{vmatrix} a_{11} & a_{12} & a_{13} \\ b_{12} & b_{22} & b_{23} \\ b_{13} & b_{23} & b_{33} \end{vmatrix} + \begin{vmatrix} b_{11} & b_{12} & b_{13} \\ a_{12} & a_{22} & a_{23} \\ b_{13} & b_{23} & b_{33} \end{vmatrix} + \begin{vmatrix} b_{11} & b_{12} & b_{13} \\ b_{12} & b_{22} & b_{23} \\ a_{13} & a_{23} & a_{33} \end{vmatrix},$$

$$e_2 = \begin{vmatrix} a_{11} & a_{12} & a_{13} \\ a_{12} & a_{22} & a_{23} \\ b_{13} & b_{23} & b_{33} \end{vmatrix} - \begin{vmatrix} b_{11} & b_{12} & b_{13} \\ a_{12} & a_{22} & a_{23} \\ a_{13} & a_{23} & a_{33} \end{vmatrix} - \begin{vmatrix} a_{11} & a_{12} & a_{13} \\ b_{12} & b_{22} & b_{23} \\ a_{13} & a_{23} & a_{33} \end{vmatrix}, \quad e_3 = \begin{vmatrix} a_{11} & a_{12} & a_{13} \\ a_{12} & a_{22} & a_{23} \\ a_{13} & a_{23} & a_{33} \end{vmatrix}.$$

fingers parameters			
k1	10	10	10
k2	1000	1000	1000
l	10	10	10
α	150	30	-90
fingers positions			
xf	-9	9	0
yf	5	5	-10
forces distribution			
Fn	1	1	1

Fig. 7. Symmetrical Grasp. Instability as a function of FIL

fingers parameters			
k1	10	10	10
k2	1000	1000	1000
l	10	10	10
α	150	30	-90
fingers positions			
xf	-9	9	0
yf	5	5	-10
forces distribution			
Fn	1	1	1

Fig. 8. Non-symmetrical Grasp. Instability as a function of FIL